PREDICTION OF HOT TEAR FORMATION IN A MAGNESIUM ALLOY PERMANENT MOLD CASTING

M. Pokorny, C. Monroe and C. Beckermann
Department of Mechanical and Industrial Engineering, University of Iowa, Iowa City, IA, USA

L. Bichler and C. Ravindran
Centre for Near-Net-Shape Processing of Materials, Ryerson University, Toronto, Ontario, Canada

Abstract

A viscoplastic deformation model considering material damage is used to predict hot tear evolution in AZ91D magnesium alloy castings. The simulation model calculates the solid deformation and ductile damage. The viscoplastic constitutive theory accounts for temperature dependent properties and includes creep and isotropic hardening. The mechanical properties are estimated from data found in the literature. Ductile damage theory is used to find mechanically induced voiding, and hot tears are expected in regions of extensive damage. Simulations are performed for a test casting consisting of a 260 mm (10.2 in) long horizontal bar connected to a vertical sprue on one side and an anchoring flange on the other. The contraction of the horizontal bar is restrained during solidification and hot tears nucleate at the junction between the horizontal bar and the vertical sprue. The hot tearing severity is manipulated by adjusting the initial mold temperature from 140°C (284°F) to 380°C (716°F). For the simulation, a trial-and-error method is used to determine the mold-metal interfacial heat transfer coefficient from experimental thermocouple results. The simulation results suggest that the predicted damage is in agreement with the hot tears observed in the experimental castings, both in terms of location and severity. The simulation results also confirm the observed decrease in hot tear susceptibility with increasing mold temperature. These results suggest that the proposed viscoplastic model with damage shows promise for predicting hot tearing.

Keywords: *hot tear, magnesium AZ91D, viscoplastic, liquidus*

Introduction

The automotive industry is showing greater interest in magnesium alloys as they have a high strength to weight ratio when compared to steel or aluminum alloys. Because of their low density, incorporating magnesium alloys into the design of new vehicles decreases weight and increases fuel efficiency. This is especially important in helping to reduce carbon emissions that contribute to global climate change. However, some magnesium alloys show a high susceptibility to hot tearing, especially if cast in a permanent mold.

Hot tears are irreversible cracks that form in the semi-solid stage, called the mushy zone, during casting[1]. The cracks may be present on the surface or in the interior of the casting. Typical surface hot tears are several millimeters long and can contribute to component failure. Hot tears develop as a result of thermal and mechanical strains due to the contraction of the casting and geometric constraints of the mold. In the mushy zone, porosity can form during late stages of solidification due to shrinkage. With sufficient deformation, this porosity may act as a nucleation site for hot tears. Hot tears can also form in the absence of porosity, but the lack of feeding flow is a necessary condition for a tear to remain open. As reviewed by Monroe and Beckermann[2], numerous attempts have been made in the past to understand the effect of various casting variables on hot tear formation and to develop criteria for predicting hot tears in castings. However, a truly predictive and reliable hot tear model is not yet available.

In the present study, a newly developed viscoplastic model that calculates deformation and damage is used to predict hot tears in AZ91D magnesium alloy castings. The model is implemented in a general purpose casting simulation code. Mechanical properties are estimated using published data. The model predictions are compared with the experimental results of Bichler *et al*[1].

Description of Experiments

Before presenting the simulation model, it is useful to briefly review the experiments of Bichler *et al*[1]. These experiments explored the hot tearing susceptibility of an AZ91D magnesium alloy test casting in a permanent steel mold. The composition of the AZ91D magnesium alloy used in the experiments was 8.61% aluminum, 0.6% zinc, 0.23% manganese, 0.017% silicon, 0.003% copper,

0.0038% iron, 0.0014% nickel, 0.0012% beryllium, and balance magnesium[1]. The casting consisted of a 260 mm (10.2 in) long horizontal bar connected to a vertical sprue and a flange, as shown in Figure 1. The figure also indicates thermocouple locations (TC1 to TC3), which recorded temperatures during casting at a rate of 7 readings/second. Temperatures of five separate castings poured at 720°C (1,328°F) were recorded using these thermocouples.

During solidification, the contraction of the horizontal bar is restrained by both the sprue and the flange. This restraint can cause hot tears to form. The hot tears always occurred at the junction of the sprue and the horizontal bar. The induced hot tearing was varied by changing the initial temperature of the steel mold. For a pouring temperature of 700°C (1,292°F), test castings were made at seven different initial mold temperatures ranging from 140°C (284°F) to 380°C (716°F). A semi-quantitative method was adopted to represent the severity of the hot tears observed in the test castings. This measure was called the hot tearing susceptibility index (HSI)[1]. As discussed in more detail below, the HSI was found to increase with decreasing initial mold temperature. In this paper, both the thermocouple results and the HSI measurements are compared to simulations.

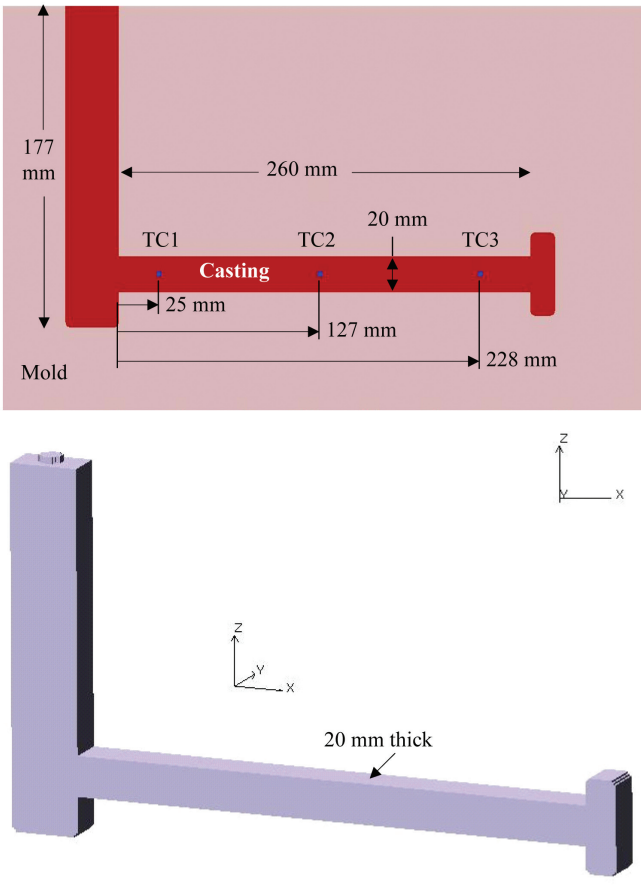

Figure 1. Casting and mold geometry with thermocouple locations.

Model

The filling, solidification and stress simulations were performed using a modified version of MAGMAsoft[3]. The simulations require inputs such as the three-dimensional geometry, mold temperature, pour temperature, thermo-physical properties, mechanical properties, mold-metal interfacial heat transfer coefficient, and others. Using these conditions and material properties, the temperature variations in both the casting and mold are predicted. The temperatures are then used in subsequent deformation calculations. Material deformation depends on the temperature results, since deformation is driven by density changes during casting solidification and further cooling within a rigid mold.

As part of the current study, a newly developed temperature-dependent viscoplastic deformation model was implemented in a module called MAGMAstress. The details of this model are rather complex, and only a brief overview is presented here. The model considers the solid and liquid phases in the mushy zone along with damage induced porosity. In the volume-averaged model for the mushy zone, the three phase fractions sum to unity, i.e.,

$$g_s + g_l + g_p = 1 \qquad (1)$$

In Equation 1, g is the local volume fraction of a phase, and the subscripts indicate the solid (s), liquid (l), and porosity (p) phases. The deformation of the mushy zone is a function of the solid fraction, which is a unique feature of the present model. Conventional models, such as the von Mises plasticity model, do not account for plastic volume change and no damage can be predicted. The model used in the current research includes the effect of plastic volume changes due to tensile (or compressive) strains.

Assuming small strain theory, the total solid strain, ε, can be decomposed into the elastic (e), thermal (th), and viscoplastic (vp) components as

$$\varepsilon = \varepsilon_e + \varepsilon_{th} + \varepsilon_{vp} \qquad (2)$$

The elastic strain is governed by Hooke's law. The thermal strain is given by the linear thermal expansion coefficient, which is calculated from the density. In the mushy zone, thermal strains are assumed to be present only for temperatures below the eutectic start temperature. The viscoplastic or creep strains are determined by the flow condition. The flow condition limits the maximum stress the material can hold by keeping the equivalent stress below the yield stress. The equivalent stress is given by

$$\sigma_{eq}^2 = A_1(g_s)q^2 + A_2(g_s)p^2 \qquad (3)$$

where σ_{eq} is the equivalent stress, q is the von Mises stress, and p is the pressure. The functions A_1 and A_2 are from the Cocks model for equivalent stress and depend on the solid

fraction[4]. In the limit where the solid fraction is unity, these functions return to the von Mises solution, where A_1 is equal to unity and A_2 is zero.

The yield stress for the fully solid material and the three-phase mixture is given by

$$\sigma_{ys} = \sigma_0 \left(1 + \frac{\varepsilon_{eq}}{\varepsilon_0}\right)^n \left(1 + \frac{\dot{\varepsilon}_{eq}}{\dot{\varepsilon}_0}\right)^m \quad (4)$$

where σ_0 is the initial yield strength, ε_{eq} is the shear plastic strain, ε_0 is the reference shear strain and is given by $\varepsilon_0 = \sigma_0 n/E$, n is the strain hardening exponent, $\dot{\varepsilon}_{eq}$ is the shear strain rate, $\dot{\varepsilon}_0$ is the reference shear strain rate, m is the strain rate sensitivity exponent, and E is the elastic modulus. The above yield stress function includes the strain rate and is therefore a creep model.

Damage due to solid deformation is porosity created by volumetric plastic strain. The volume fraction damage (porosity) is found by integrating over time the volumetric part of the viscoplastic strain rate as

$$g_p = \int_{t_{cr}}^{t} g_s \,\mathrm{tr}\left(\dot{\boldsymbol{\varepsilon}}_{\mathrm{vp}}\right) dt \quad (5)$$

where t is time, t_{cr} is the time when damage begins to accumulate, and tr() is the trace operation function for the volumetric contribution of the inelastic strains. For simplicity, the critical time is taken as the beginning of the simulation. It should be noted, that the predicted damage is only an indicator of where hot tears may form in a casting; it does not predict the exact shape or size of the final hot tear. The potential for hot tearing increases with an increase in magnitude of this damage indicator. Damage provides an estimate of the volume that the crack occupies.

Thermo-physical and Mechanical Properties

Some of the properties of the AZ91D alloy needed in the simulations were determined using the thermodynamic software package JMatPro[5]. They include the solid fraction, density, thermal conductivity, specific heat and latent heat, all as a function of temperature. The composition of the alloy used to generate these properties is the same as the experimental composition but with the nickel and beryllium left out, because the software package does not offer these elements in the magnesium database. The properties were calculated using a Scheil analysis with a 1% cutoff. The predicted liquidus, eutectic start, and 100% solid temperatures are equal to 603°C (1,117°F), 431°C (808°F), and 403°C (757°F), respectively. The fact that the 100% solid temperature (with a 1% cutoff) is 28°C (51°F) below the eutectic start temperature indicates that the eutectic ($Mg_{17}Al_{12}$) does not form isothermally. The thermodynamic software package also predicts the formation of small amounts of additional phases (Mg_2Si and Al_4Mn) near the end of solidification.

The mechanical properties, including the elastic and viscoplastic properties, were estimated from stress-strain curves found in the literature[6-20]. These stress-strain curves cover a range of temperatures and strain rates. Data from AZ91 alloy designations A-E, as well as various heat treatments and casting processes (die, permanent mold, and sand cast), were drawn upon. This wide range of data was used because a complete set of stress-strain curves for AZ91D, covering the full range of temperatures and strain rates encountered during casting, is not available. As a result, the mechanical properties should be considered preliminary estimates only.

The Young's elastic modulus curve used in the simulations is shown in Figure 2(a). The estimated modulus decreases linearly from 46.0 GPa at room temperature to 20.0 GPa at 100% solid[6]. Through the solidification temperature interval, the following solid fraction dependent relation based on the study of Roberts and Garboczi[21] was used

$$E = E_s \left(\frac{g_s - g_s^E}{1 - g_s^E}\right)^{n^E} \quad (6)$$

Equation (6) shows that Young's elastic modulus for the solid material, E_s, is multiplied by a factor between zero and unity, thus reducing the effective modulus, E, for the three-phase mixture when the solid fraction is below unity. When the solid fraction is below the critical solid fraction g_s^E, the modulus is set to a negligibly small value, signifying that there is not enough solid in the mushy zone to support any stress. According to a previous study on the stiffness of a porous metal alloy,[22] the critical solid fraction was taken as 0.5 and the power coefficient, n^E, as 2.5. For the Poisson's ratio, no temperature dependent data was found, so a constant value of 0.35 was used from room temperature to 100% solid[7,8]. Through the solidification temperature interval, the following solid fraction dependent relation from Roberts and Garboczi[21] was used

$$\nu = \nu_0 + \left(\frac{g_s - g_s^\nu}{1 - g_s^\nu}\right)(\nu_s - \nu_0) \quad (7)$$

Equation (7) shows that the Poisson's ratio for the solid material, ν_s, is scaled from the fully solid value to a minimum Poisson's ratio, ν_0. This scaling occurs over a solid fraction range between unity and g_s^ν. The critical solid fraction for the Poisson's ratio, g_s^ν, is given by 0.52, and the minimum Poisson's ratio by 0.14[21]. The resulting temperature dependent Poisson's ratio curve is shown in Figure 2(b).

The viscoplastic properties estimated from the available stress-strain curves are shown in Figures 2(c) and 2(d). The initial yield stress, σ_0, and the strain hardening exponent, n, decrease with increasing temperature. The strain rate sensitivity exponent, m, increases with increasing

temperature, indicating rate independent behavior at low temperatures and rate dependent or creep behavior at high temperatures. The reference strain rate was set to a constant equal to 10^{-5} 1/s; this value is only approximate due to a lack of experimental data. Using all of the regressed parameters, the stress can be calculated at a given temperature, strain, and strain rate. Figure 3(a) shows a comparison of predicted stresses to measured stresses from the various stress-strain curves found in the literature[6-20]. Due to the large variety of sources used in the present study, some scatter can be observed. In Figure 3(b), a particular predicted stress-strain curve is compared to experimental stress-strain data. The curve shows reasonable agreement in both yielding and hardening behavior.

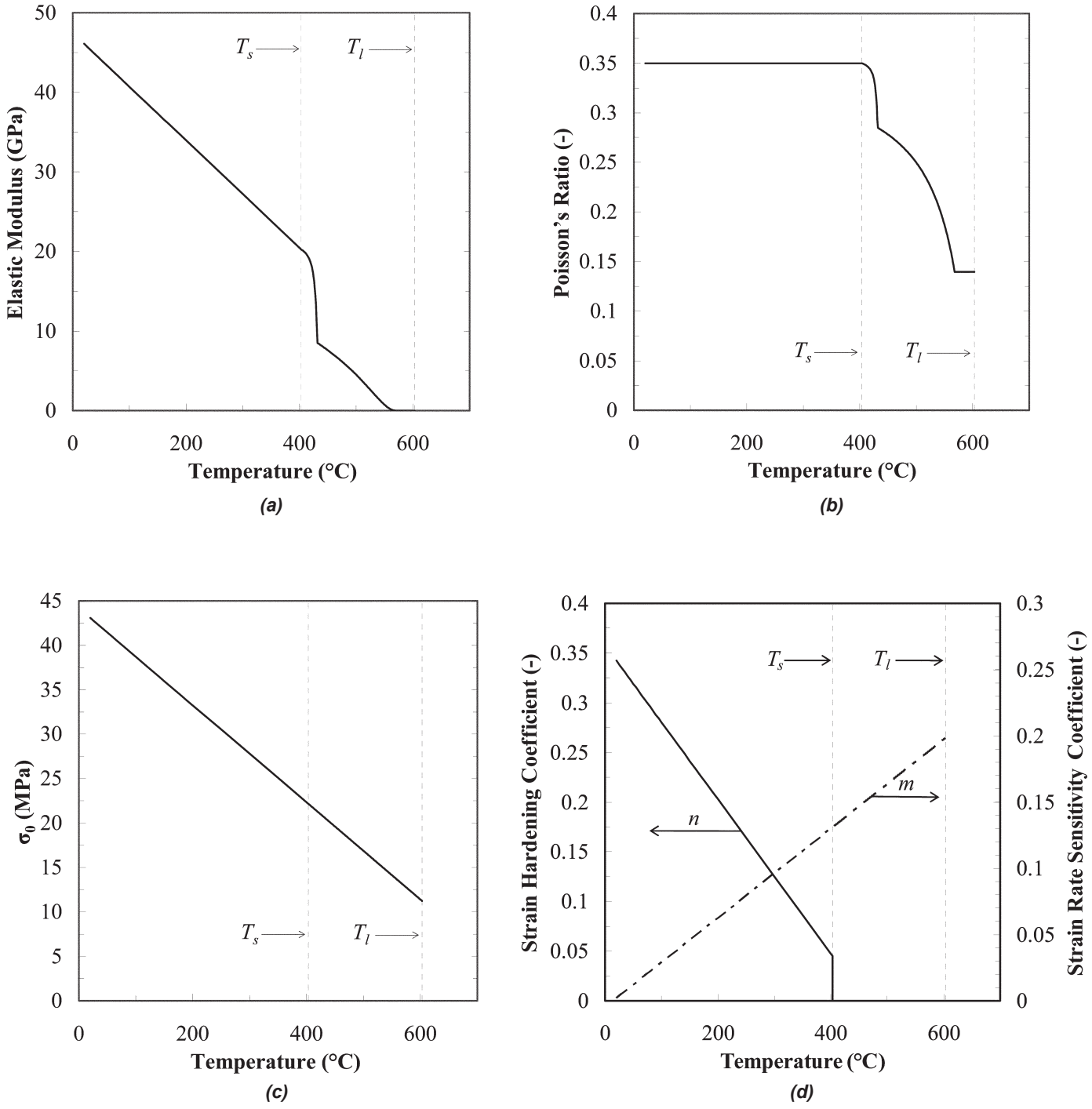

Figure 2. Mechanical properties used in the hot tear simulation: (a) Young's elastic modulus; (b) Poisson's ratio; (c) initial yield strength; (d) strain hardening and strain rate sensitivity coefficients.

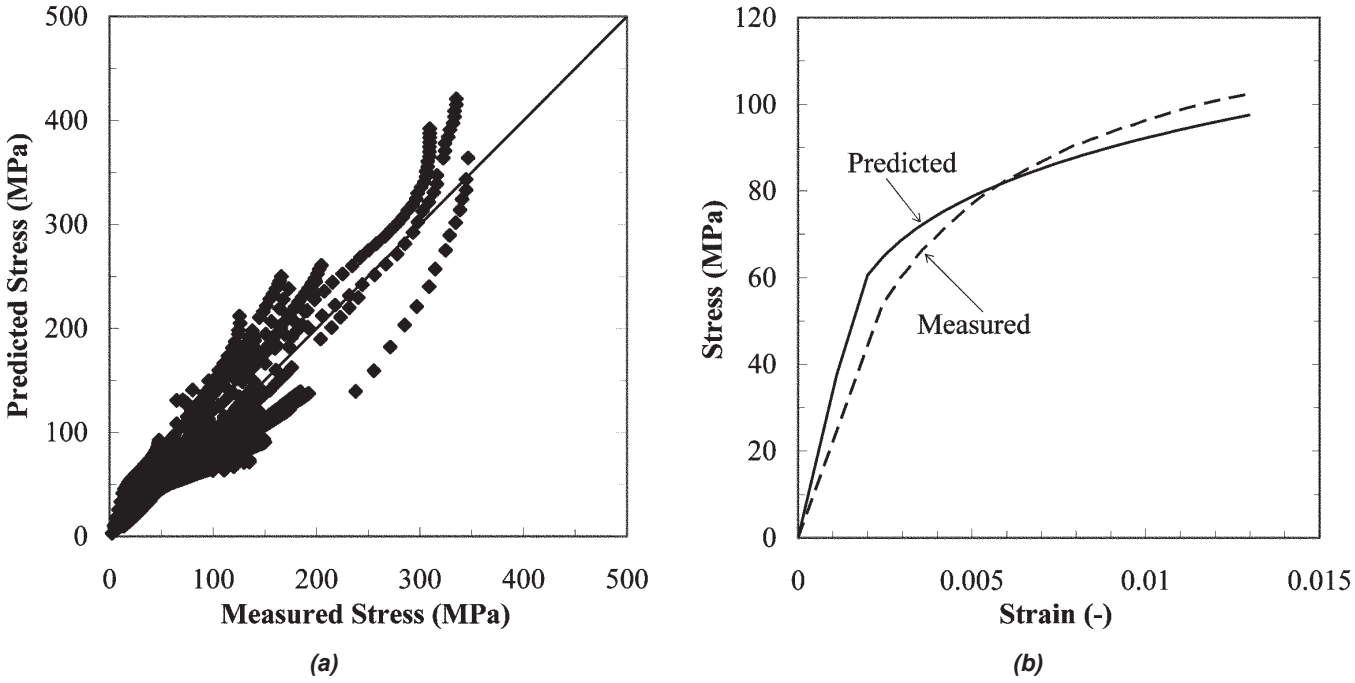

Figure 3. Comparison of predicted stresses and measured stresses: (a) plot of total predicted stress and experimentally measured stress,[9-20] with a solid line indicating a perfect fit [temperature range of 20°C (68°F) to 370°C (698°F) and strain rate range of 5.7X10^{-7} to 8.3X10^{-2} 1/s]; (b) example stress-strain plot for one experiment[10] and the predicted stress [at 204°C (399°F) and a strain rate of 1.8X10^{-4} 1/s].

Results

Temperature Predictions

The temperature measurements were used to determine the mold-metal interfacial heat transfer coefficient and to confirm the accuracy of the solidification and heat transfer simulations. The heat transfer coefficient was obtained using a trial-and-error procedure in which the predicted temperatures were matched with the experimental thermocouple data. The resulting heat transfer coefficient variation with temperature is shown in Figure 4(a). Above the liquidus temperature, a heat transfer coefficient of 6000 W/m^{2}K was found to result in good agreement between measured and predicted temperatures. Through the solidification range, the heat transfer coefficient was varied with the solid fraction to a final value of 1000 W/m^{2}K at 100% solid. From 100% solid to room temperature, the heat transfer coefficient was decreased cubically to 100 W/m^{2}K. The decrease in the heat transfer coefficient with temperature reflects the formation of an air gap between the casting and the mold during cooling.

Figure 4(b) shows an example of a measured and predicted temperature comparison. Temperature versus time curves are shown for a thermocouple indicated as TC1 in Figure 1. The measured and predicted temperatures can be seen to be in generally good agreement. Similar agreement was obtained for all experiments in which temperatures were measured.

More insight can be obtained by examining the measured and predicted cooling rate curves that are also shown in Fig. 4(b). The cooling rate curves were obtained using a five point moving average of the time derivative of the temperature data. The first major peak in the measured cooling rate curve indicates nucleation of the primary Mg-rich solid. The peak corresponds to a temperature of 598°C (1,108°F) (average value from all temperature measurements). This nucleation temperature is 5°C (9°F) below the liquidus temperature of 603°C (1,117°F) predicted by the thermodynamic software. The difference may be attributed to the presence of some nucleation undercooling; in fact, a temperature recalescence can be observed in the measurements. Nucleation is not modeled by the thermodynamic software package. A second major peak in the cooling rate curve indicates the start of eutectic solidification. The measured eutectic start temperature is equal to 421°C (790°F) (average value from all temperature measurements). This value is 10°C (18°F) lower than the eutectic start temperature start temperature. The difference may be attributed to inaccuracies in the thermodynamic software, in particular the Scheil analysis used to model solidification and the neglect of eutectic undercooling. The final 100% solid temperature cannot be inferred from the measured and predicted cooling rate curves due to the absence of any discernible peak. Despite the inaccuracies in the data obtained from the thermodynamic software package, the agreement between the measured and predicted temperatures was still deemed satisfactory for the present purposes.

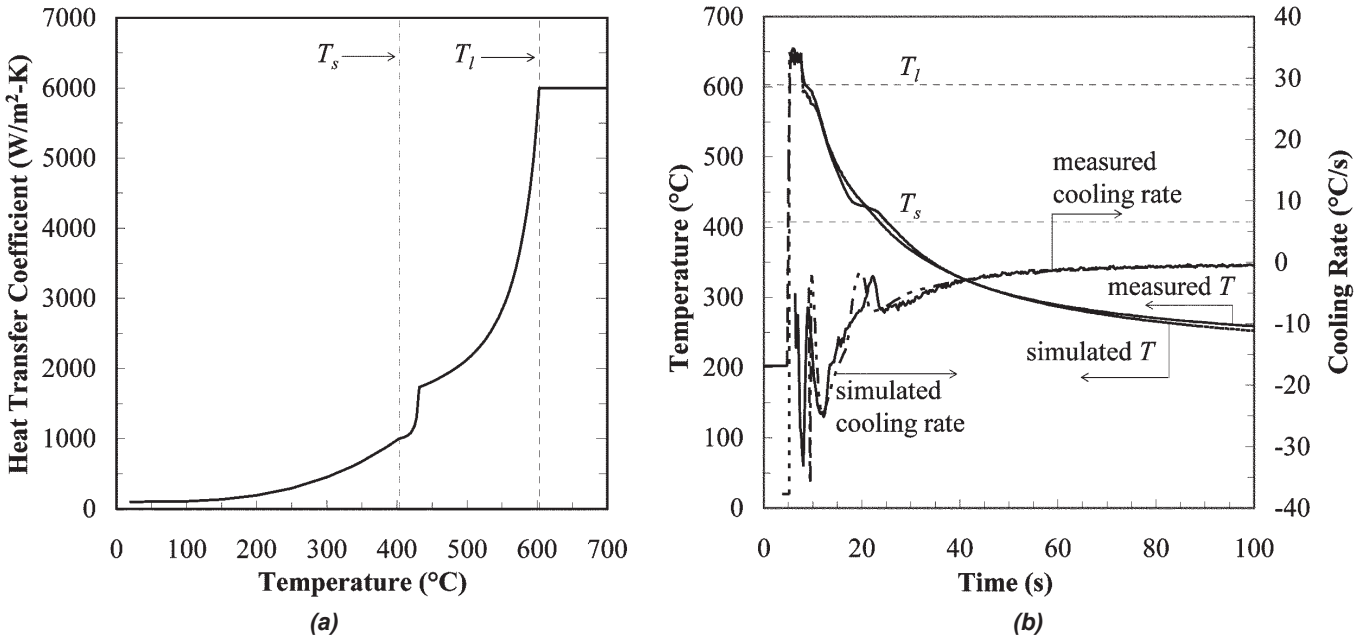

Figure 4. Interfacial heat transfer coefficient and thermocouple results: (a) final interfacial heat transfer coefficient as a function of temperature; (b) measured and simulated thermocouple results for TC1 and an initial mold temperature of 202°C (396°F).

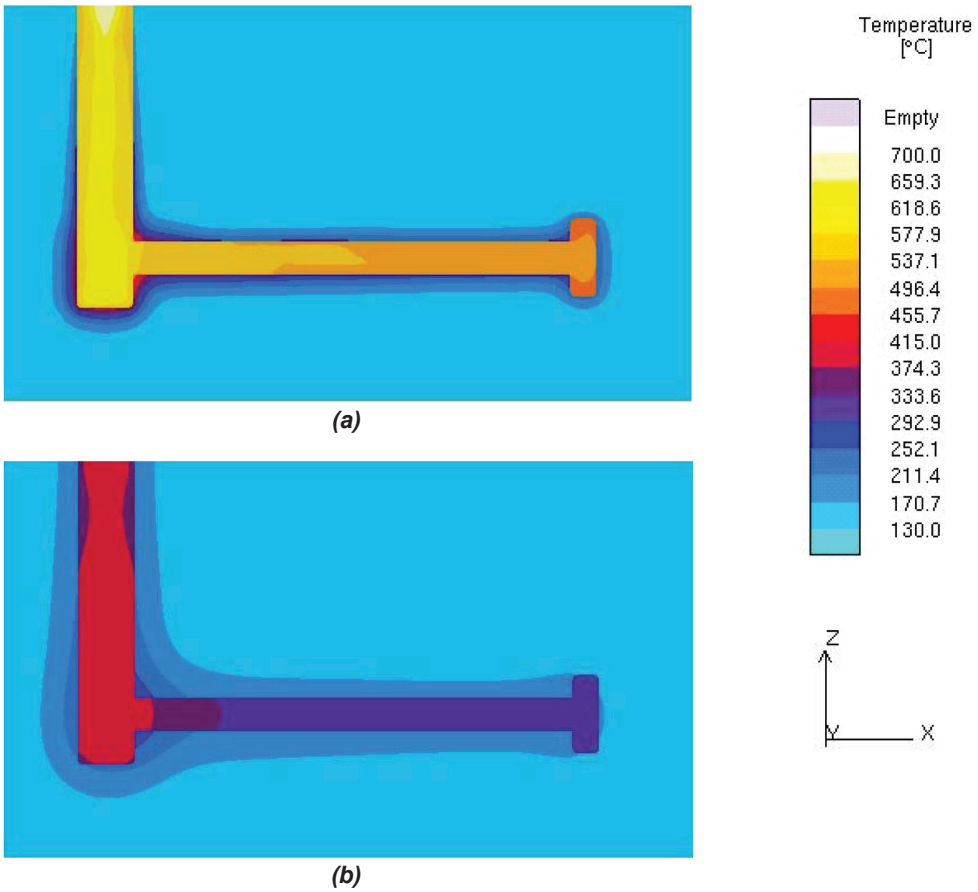

Figure 5. Calculated temperature fields for both the mold and the casting for an initial mold temperature of 140°C (284°F): (a) temperature field at the end of filling; (b) temperature field at 100% solid.

Figure 5 shows predicted temperature fields for both the mold and the casting immediately after filling and at 100% solid. These results show that the heat from the casting propagates into the mold as expected. A relatively large temperature gradient can be observed in the casting near the junction between the sprue and the horizontal bar. The sprue and the horizontal bar are both fairly isothermal, but the sprue temperature remains about 80°C higher than the bar temperature. The combination of the hot sprue and the early solidification of the bar leads to large thermal strains and, depending on the initial mold temperature, to the formation of a hot tear at the junction between the sprue and the horizontal bar.

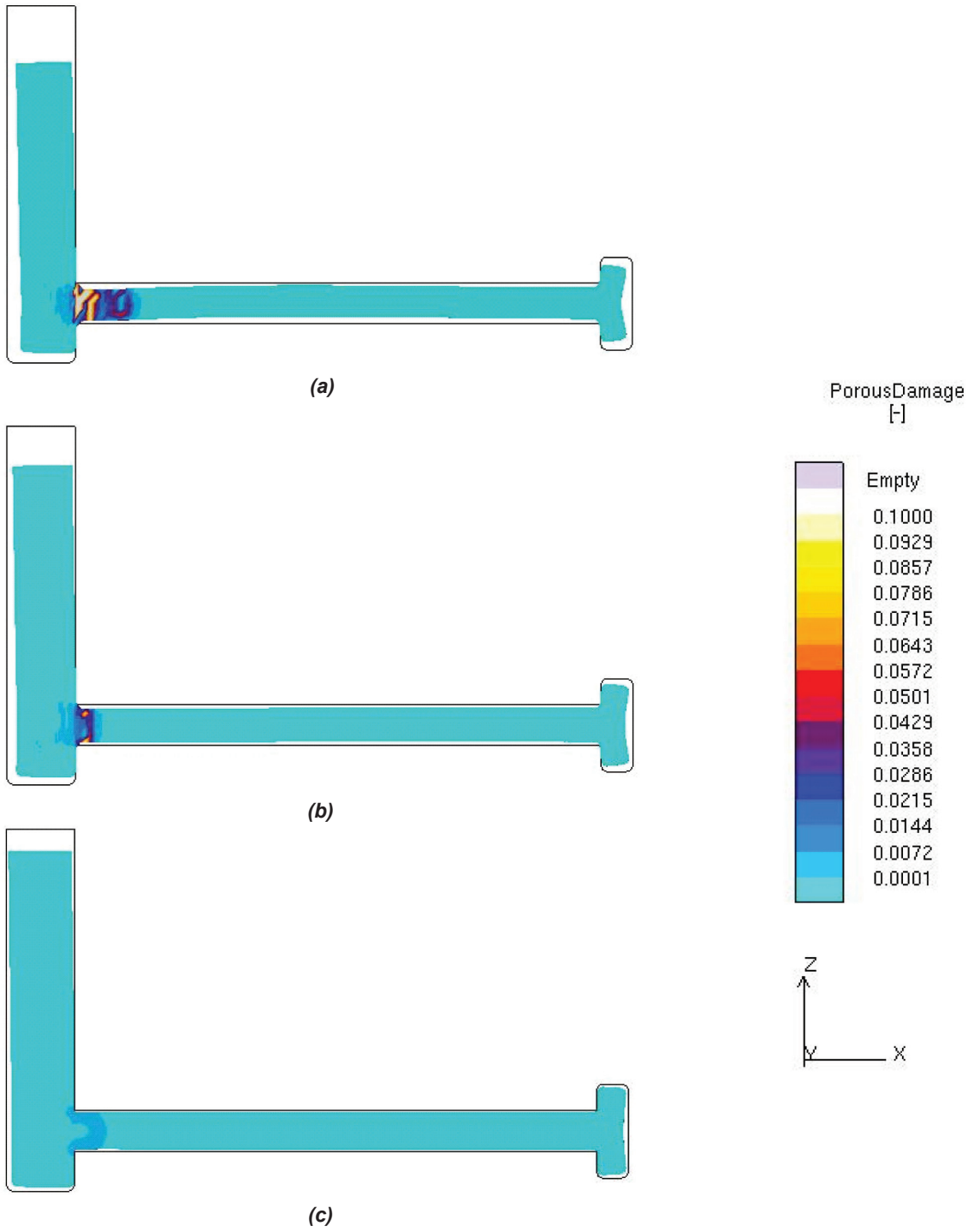

Figure 6. Calculated distortion of the casting magnified 20 times: (a) initial mold temperature of 140°C (284°F); (b) initial mold temperature of 260°C (500°F); (c) initial mold temperature of 380°C (716°F).

Deformation and Hot Tear Predictions

Model predictions are compared to experimental results for three mold temperatures, 140°C (284°F), 260°C (500°F) and 380°C (716°F), and a pouring temperature of 700°C (1,292°F). Figure 6 shows the calculated final damage field and distortion of the casting magnified by 20 times for the three different initial mold temperatures. The simulations were terminated at 350 sec. after pouring; at this time the casting was fully solid and at a temperature close to the initial mold temperature. In Figure 6, the solid black line represents the original non-deformed casting. It can be seen that the sprue undergoes free contraction along its height. The magnitude of the contraction decreases with increasing initial mold temperature, since the thermal strain is less for a smaller temperature interval between the end of solidification and the final casting temperature (which is approximately given by the initial mold temperature). Several contact points can be observed along the mold-metal interface, which provide the necessary restraint for deformation and hot tears to occur. The most important contact points are seen at the junction of the sprue and the bar and at the flange end. Although the entire bar experiences contraction and restraint, the deformation causes the most significant damage on the sprue side of the bar. As expected, more damage (and distortion) is predicted to occur as the initial mold temperature is decreased.

Figure 7 shows the calculated von Mises stress and plastic effective strain at the end of the simulation for an initial mold temperature of 260°C (500°F). The von Mises stress is largest in the bar and almost zero in the sprue, as can be seen in Figure 7(a). In Figure 7(b), the plastic effective strain can be seen to be large in the bar with the largest values near the corners at the flange end. Hence, a hot tear criterion based on a von Mises model and effective strain alone would predict hot tear formation at the flange end where the stress and effective plastic strain are highest. However, in the experiments the hot tears did not form at the flange end, but at the junction with the sprue. Therefore, a prediction based on the von Mises stress and effective plastic strains would be inadequate for this casting.

Figure 8 shows a comparison between the predicted damage fields and photographs of the hot tears formed in the experiments for the three mold temperatures[1]. In Figure 8, the graphs with the simulation results were rotated by 180° so that the sprue is now to the right of the horizontal bar. This rotation is done in order to match the view in the photographs. It can be seen that the predicted damage is at the same location where the hot tears occurred in the experiments. The strong increase in the calculated damage with decreasing mold temperature corresponds well with the increasing severity of the hot tears seen in the experimental results.

In order to compare the hot tear predictions with the HSI introduced by Bichler *et al*.,[1] the calculated damage is summed over the volume of the casting to give a value for the total damage. The total volume of damage is then divided by the total casting volume to give a percent of the casting with damage. The percentage of damage and the HSI are not directly comparable, but they are both a measure of the hot tear severity. Figure 9 shows plots of the HSI values from the experiments[1] and the total percentage of damage obtained from the present simulations, both as a function of the initial mold temperature. The curve generated from the simulation results [Figure 9(b)] shows a similar trend as the 700°C (1,292°F) line on the HSI plot [Figure 9(a)]. Hence, these simulation results confirm the observed decrease in hot tear susceptibility with increasing mold temperature.

Conclusions

A new viscoplastic deformation model was used to predict hot tears in an AZ91D magnesium alloy permanent mold casting. The model calculates deformation and material damage. Preliminary estimates of temperature and strain rate dependent mechanical properties were obtained from stress-strain data found in the literature. Simulations were performed of experimental test castings of Bichler *et al*.[1] The predicted damage from the simulations was found to be in good agreement with the hot tears observed in the experiments, both in terms of location and severity. The simulation results corroborate that the hot tears form most likely at the junction between the horizontal bar and the vertical sprue. The simulation results also confirm that hot tear susceptibility decreases with increasing mold temperature. These results indicate that the damage calculated using the new viscoplastic deformation model is a reasonable predictor of hot tearing. Future work will include the measurement of more accurate mechanical properties and the coupling of the deformation model with shrinkage porosity simulation. In addition, it will be desirable to compare the predicted stresses and strains with direct experimental measurements.

Acknowledgments

The authors would like to thank Joseph Carpenter (United States Department of Energy) who funded the modeling aspects of this work under the High Integrity Magnesium Cast Components (HIMAC) Project, and USAMP for approving the work.

The authors would also like to thank the HIMAC team of Bruce Cox (Chrysler LLC), Chair, Larry Quimet and Alan Luo (General Motors Corporation), Jacob Zindel (Ford Motor Company), Steve Robison (AFS), David Weiss (Eck Industries) and the project administrator D. E. Penrod (Manufacturing Services and Development Inc). The authors greatly appreciate the support provided by Magma Foundry Technologies Inc.

The authors are grateful to the Natural Sciences and Engineering Research Council of Canada (NSERC) for supporting the experimental aspects of this work through a Canada Graduate Scholarship (Bichler) and a Discovery Research Grant (Ravindran). Also, they sincerely acknowledge valuable assistance from A. Machin in carrying out the experiments.

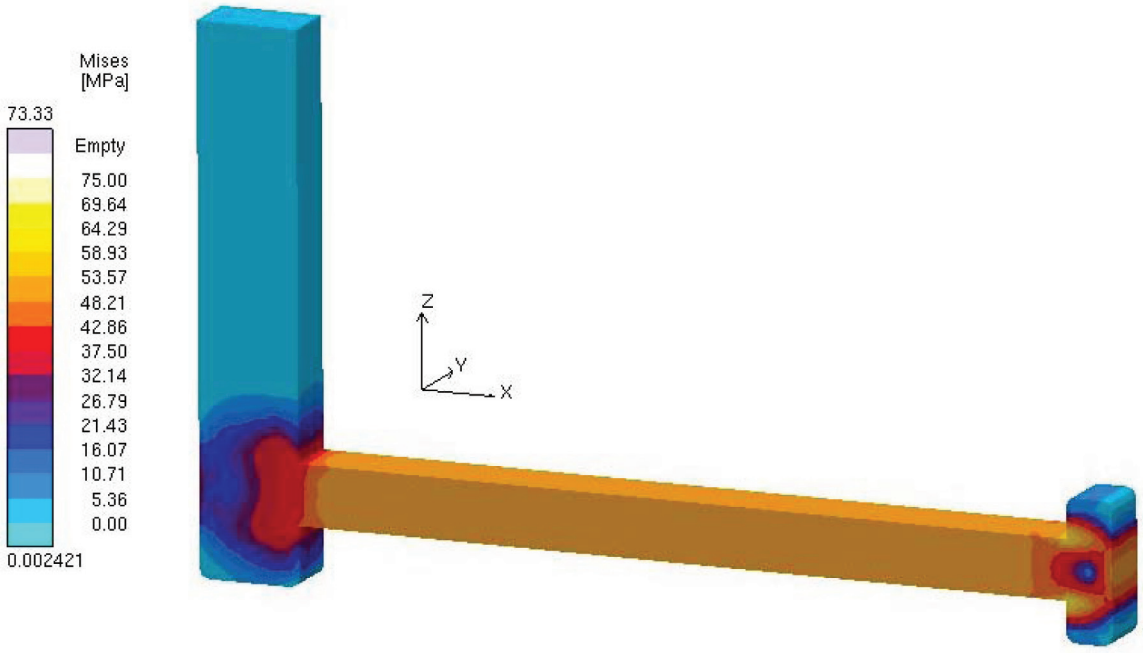

(a)

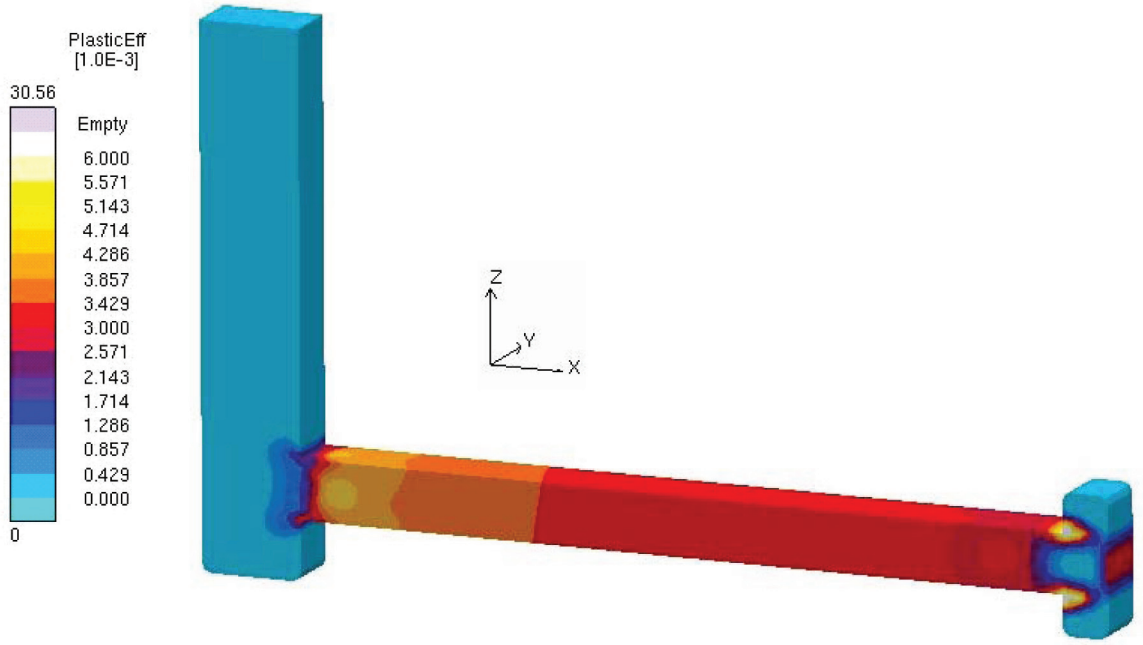

(b)

Figure 7. Stress and strain results at the end of the simulation, 350s, for an initial mold temperature of 260°C (500°F): (a) calculated von Mises stress; (b) calculated plastic effective strain.

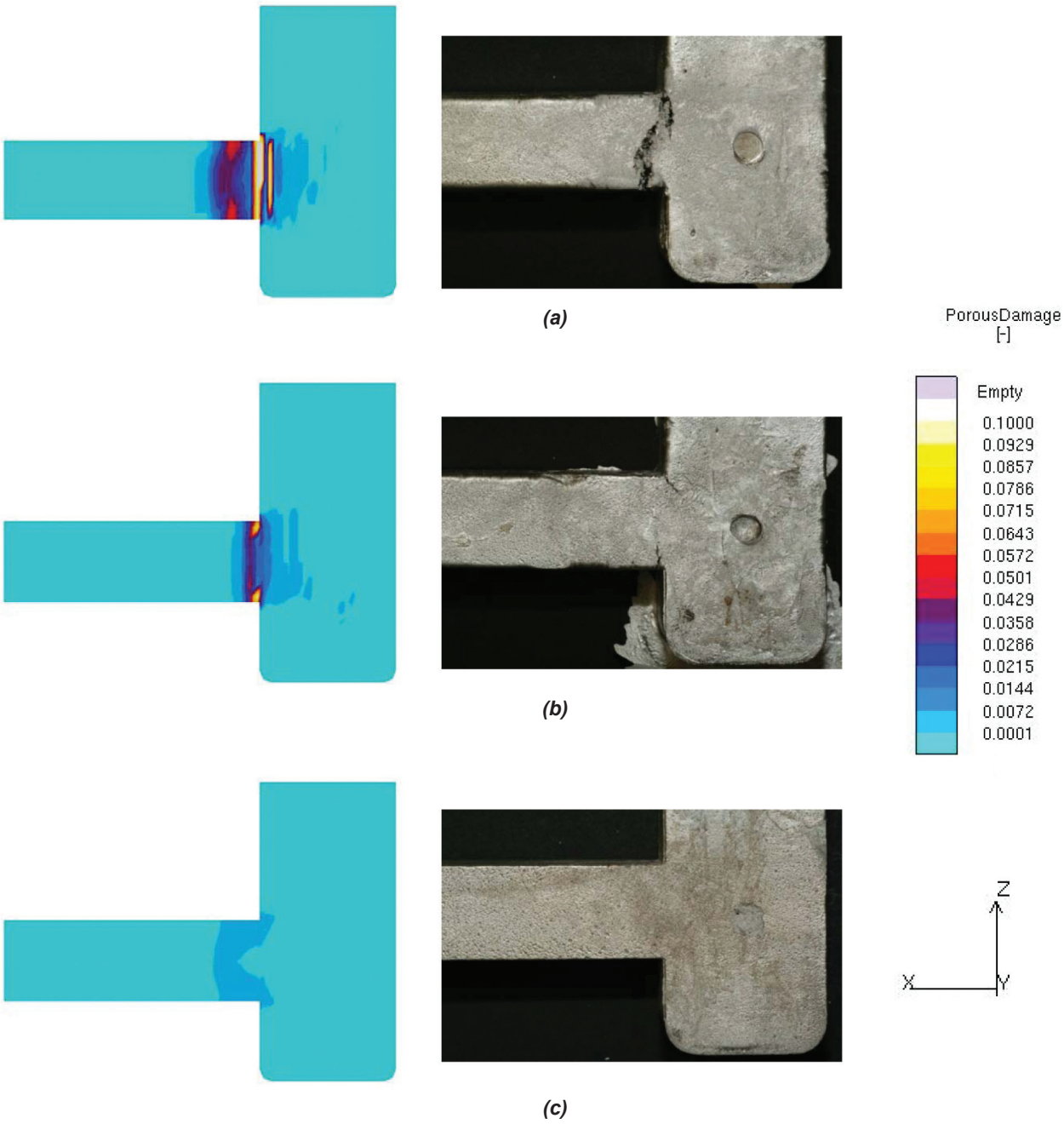

Figure 8. Simulation results showing calculated damage and the corresponding experimental results[1]: (a) initial mold temperature of 140°C (284°F); (b) initial mold temperature of 260°C (500°F); (c) initial mold temperature of 380°C (716°F).

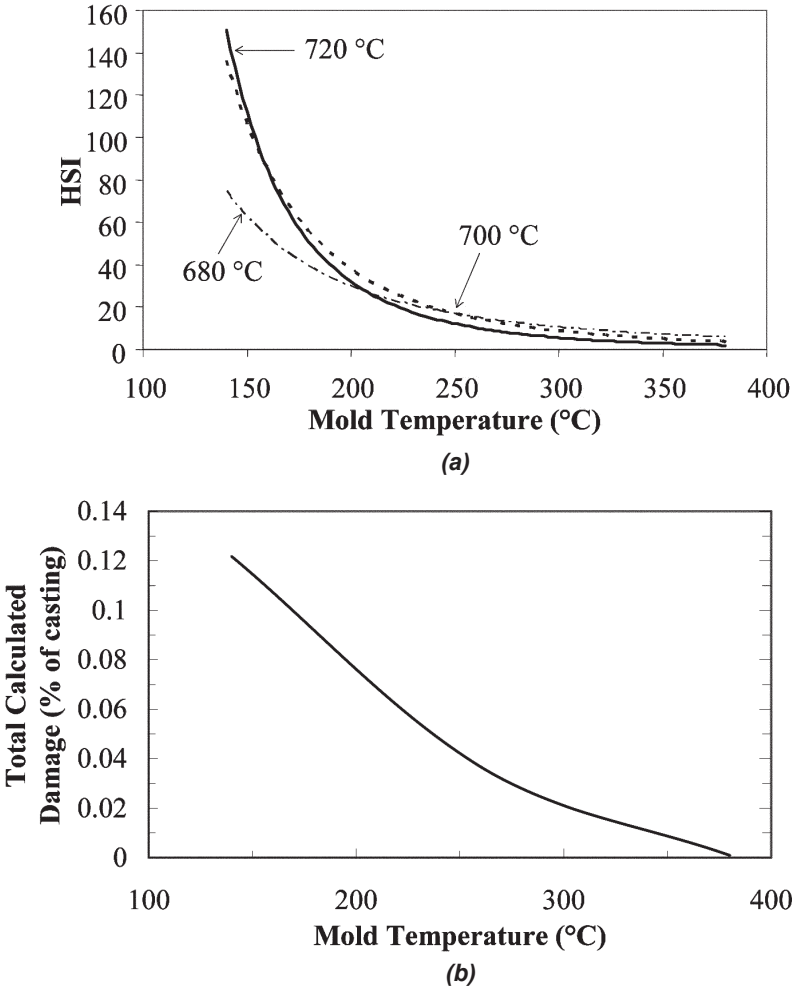

Figure 9. Hot tear susceptibility and calculated total damage at various mold temperatures: (a) HSI values from experimental results[1]; (b) calculated total damage from simulation results.

Disclaimer

This material is based upon work supported by the Department of Energy National Energy Technology Laboratory under Award Number DE-FC26-02OR22910. This report was prepared as an account of work sponsored by an agency of the United States Government. Neither the United States Government nor any agency thereof, nor any of their employees, makes any warranty, express or implied, or assumes any legal liability or responsibility for the accuracy, completeness, or usefulness of any information, apparatus, product, or process disclosed, or represents that its use would not infringe privately owned rights. Reference herein to any specific commercial product, process, or service by trade name, trademark, manufacturer, or otherwise does not necessarily constitute or imply its endorsement, recommendation, or favoring by the United States Government or any agency thereof. The views and opinions of authors expressed herein do not necessarily state or reflect those of the United States Government or any agency thereof.

REFERENCES

1. Bichler, L., Elsayed, A., Lee, K., and Ravindran, C., "Influence of Mold and Pouring Temperatures on Hot Tearing Susceptibility of AZ91D Magnesium Alloy," *International Journal of Metalcasting* , vol. 2, no. 1, pp 43-56 (2008).
2. Monroe, C., and Beckermann, C., "Development of a Hot Tear Indicator for Steel Castings," *Materials Science and Engineering A*, vol. 413-414, pp 30-36 (2005).
3. MAGMAsoft, MAGMA GmbH, Kackerstrasse 11, 52072 Aachen, Germany.
4. Marin, E.B., and McDowell, D.L., "A Semi-implicit Integration Scheme for Rate-dependent and Rate-independent Plasticity," *Computers and Structures*, vol. 63, no. 3, pp 579-600 (1997).
5. JMatPro, Sente Software Ltd., Surrey Technology Centre, Surrey GU2 7YG, United Kingdom.
6. Dow Chemical Company, "AZ91A-F Die Castings. R.R. Moore Fatigue Curves," *Technical Service and Development Letter Enclosure* (1957).

7. Hutchinson, C.R., Nie, J.F., and Gorsse, S., "Modeling the Precipitation Processes and Strengthening Mechanisms in a Mg-Al-(Zn) AZ91 Alloy," *Metallurgical and Materials Transactions A*, vol. 36A, pp 2093-2105 (2005).
8. Uchida, S., Takeuchi, I., Gonda, G., Hirai, K., Uesugi, T., Takigawa, Y., and Higashi, K., "Mechanical Properties of Twin Roll Cast AZ91 Magnesium Alloy at Room Temperature," *Advanced Materials Research*, vols. 26-28, pp 145-148 (2007).
9. ASTM Specification B 199, "Standard Specification for Magnesium-alloy Permanent Mold Castings," *Annual Book of ASTM Standards*, vol. 02.02, sec.2 (1984).
10. Fenn, R.W.Jr., and Gusack, J.A., "Effect of Strain-rate and Temperature on the Strength of Magnesium Alloys," *ASTM Proceedings* 58:685 (1958).
11. Ishikawa, K., Watanabe, H., and Mukai, T., "High Strain Rate Deformation Behavior of an AZ91 Magnesium Alloy at Elevated Temperatures," *Materials Letters*, vol. 59, pp 1511-1515 (2005).
12. Ma, Y.Q., Chen, R.S., and Han, E., "Development of a High Strength and High Ductility Magnesium Alloy," *Materials Science Forum*, vols. 488-489, pp 265-268 (2005).
13. Caceres, C.H., Davidson, C.J., Griffiths, J.R., and Newton, C.L., "Effects of Solidification Rate and Ageing on the Microstructure and Mechanical Properties of AZ91 Alloy," *Materials Science and Engineering A*, vol. 325, pp 344-355 (2002).
14. Cavaliere, P., and De Marco, P.P., "Superplastic Behaviour of Friction Stir Processed AZ91 Magnesium Alloy Produced by High Pressure Die Cast," *Journal of Materials Processing Technology*, vol. 184, pp 77-83 (2007).
15. Ding, W., Jin, L., Lin, D., Zeng, X., and Mao, D., "Effect of Second Phase on the Mechanical Properties of Mg-Al-Zn Alloy by Equal Channel Angular Extrusion," *Materials Science Forum*, vols. 546-549, pp 249-252 (2007).
16. Mabuchi, M., Kobata, M., Chino, Y., and Iwasaki, H., "Tensile Properties of Directionally Solidified AZ91 Mg Alloy," *Materials Transactions*, vol. 44, no. 4, pp 436-439 (2003).
17. Zhao, M., Liu, M., Song, G., and Atrens, A., "Influence of Homogenization Annealing of AZ91 on Mechanical Properties and Corrosion Behavior," *Advanced Engineering Materials*, vol. 10, no. 1-2, pp 93-103 (2008).
18. Watanabe, H., Ishikawa, K., and Mukai, T., "High Strain Rate Deformation Behavior of Mg-Al-Zn Alloys at Elevated Temperatures," *Key Engineering Materials*, vols. 340-341, pp 107-112 (2007).
19. *Aerospace Structural Metals Handbok*, Vol. 3, Code 3402, CINDAS/USAF CRDA Handbooks Operation, Purdue University, p. 12 (1995).
20. *Military Handbook*, MIL-HDBK-5H: Metallic Materials and Elements for Aerospace Vehicle Structures, US Department of Defense, Ch. 4, p. 32 (1998).
21. Roberts, A.P., and Garboczi, E.J., "Elastic Properties of Model Porous Ceramics," *Journal of the American Ceramic Society*, vol. 83, no. 12, pp 3041-3048 (2000).
22. Hardin, R. A., and Beckermann, C., "Effect of Porosity on the Stiffness of Cast Steel," *Metallurgical and Materials Transactions A,* vol. 38, pp 2992-3006 (2007).

Prediction of Hot Tear Formation in a Magnesium Alloy Permanent Mold Casting

M.Pokorny, C.Monroe, C. Beckermann, University of Iowa, Iowa City, IA, USA
L. Bichler, C. Ravindran, Ryerson University, Toronto, Ontario, Canada

Reviewer: The solidus temperature (403°C) as predicted by JMatPro seems to be much lower than expected for AZ91D. Could the authors comment on this calculated value, and the possible effect on the results of a higher value for the solidus temperature?

Authors:*The value of 403 C is not the (equilibrium) solidus temperature (note: JMatPro gives an equilibrium solidus temperature of 442 C for this alloy), but the result of a non-equilibrium Scheil calculation with a 1% cutoff. As noted later under Temperature Predictions, the measured eutectic start temperature is 421 C. This value is not only below the equilibrium solidus temperature (442 C), as expected, but also 10 C below the predicted eutectic start temperature from JMatPro (431 C). The 100% solid temperature from the Scheil analysis (403 C) is below the eutectic start temperature, because the eutectic does not form isothermally. In fact, solidification is predicted to conclude not only with the formation of the eutectic ($Mg_{17}Al_{12}$), but also with small amounts of Mg_2Si and Al_4Mn phases. Hence, the predicted 100% solid temperature is in fact not "much lower than expected". In no case should one expect a 100% solid temperature above the measured eutectic start temperature of 421 C. Sentences have been added to the manuscript to explain that the eutectic does not form isothermally. Other items above were already mentioned in the manuscript.*

Reviewer: *"The strain rate exponent, m, increases….. high temperatures"* does seem to be a bit contradictory in that "m" is shown in Fig. 20(d) to be a linear function of temperature throughout, at both low and high values. Any comment from the authors?

Authors: *The reviewer may have misread this sentence. The strain rate sensitivity exponent indeed increases linearly with temperature. A low value at low temperature implies rate independent behavior, and a high value at high temperature means that rate-dependent or creep behavior is important.*

Reviewer: The authors are to be congratulated for deriving the metal-mold HTC for their solidification model rather than using standard MAGMA data. Boron nitride coating is not very insulating, so we would expect a high initial value for the HTC at contact with the molten metal. However, a value of 6000 W/m2K seems quite high.

Authors: *The value of 6,000 W/m^{2}K is not too high. About 15 years ago we measured HTCs for a liquid metal in contact with a coated metal mold that were as high as 8,000 to 10,000 W/m^{2}K [Reddy, A.V., and Beckermann, C., "Measurements of Metal-Mold Interfacial Heat Transfer Coefficients during Solidification of Sn and Sn-Pb Alloys," Experimental Heat Transfer, Vol. 6, 1993, pp. 111-129.] The entire topic of how we determined the HTCs in the present study deserves more discussion. However, due to space limitations and because this is not central to the present topic of hot tears, we would prefer not to discuss this in any greater detail than already done in the manuscript.*